The effect of viscoelasticity on the extrusion drawing in film-casting process

Article *in* Rheologica Acta · July 2010

DOI: 10.1007/s00397-010-0454-9

5 authors, including:

Seiji Shiromoto
Sumitomo Chemical
31 PUBLICATIONS **103** CITATIONS

SEE PROFILE

Rheol Acta (2010) 49:757–767
DOI 10.1007/s00397-010-0454-9

ORIGINAL CONTRIBUTION

The effect of viscoelasticity on the extrusion drawing in film-casting process

Seiji Shiromoto · Yasushi Masutani · Masaaki Tsutsubuchi · Yoshiaki Togawa · Toshihisa Kajiwara

Received: 16 June 2009 / Revised: 23 February 2010 / Accepted: 10 April 2010 / Published online: 29 April 2010

Abstract The governing rheological property for extrusion drawing in film-casting process is proposed in this study. The experiment of film-casting process using the high-pressure process low-density polyethylene (LDPE) was performed. The non-isothermal viscoelastic simulation of the film casting experiment was also carried out to explain the experimental results. Film width reduction phenomenon in an air gap, so-called neck-in behavior, was investigated by using the simulation of the LDPE and the model fluids exhibiting specific viscoelasticity. The neck-in phenomenon was also examined using theoretical model based on force balance and deformation type of a film. As a result, the neck-in normalized by the air gap was in good correlation with the ratio of planar to uniaxial elongational viscosity rather than the strain hardening nature of uniaxial elongational viscosity.

Keywords Film casting · Neck-in · Air gap · Uniaxial elongational viscosity · Planar elongational viscosity

S. Shiromoto (✉) · Y. Masutani · M. Tsutsubuchi · Y. Togawa
Sumitomo Chemical Co., Ltd., 2-1 Kitasode,
Sodegaura, Chiba 299-0295, Japan
e-mail: shiromoto@sc.sumitomo-chem.co.jp

T. Kajiwara
Department of Chemical Engineering, Kyushu University,
744 Motooka, Nishi-ku, Fukuoka 819-0395, Japan

Introduction

The film casting is an industrially important process for producing various films because films has been used in the wide range of application areas and the amount of the film products consumption continues growing. In film-casting process, molten polymer is extruded in film shape through thin gap of a flat die. The extruded molten polymer is highly stretched along flow direction due to higher take-up velocity than extruded velocity, while film width decreases. This film width reduction phenomenon is called neck-in. Film width reduction by extrusion drawing causes thicker film edge, so called edge-bead. The neck-in and edge-bead phenomenon strongly depends on the viscoelasticity of the materials and the processing conditions. From an industrial point of view, these defects have to be suppressed because they reduce productivity and properties of the products. Therefore, the understanding of the effect of viscoelasticity on the neck-in phenomenon is important in controlling film casting process.

Many simulations of film casting process have employed viscous fluid and quasi three-dimensional finite element model (D'Halewyn et al. 1990; Barq et al. 1992; Smith and Stolle 2003; Sollogoub et al. 2003). Full three-dimensional flow simulation was first performed by Sakaki et al. (1996). The simulation results using Newtonian fluid were in good agreement with the experimental data for a high-density polyethylene film. They reported that the neck-in depended on air gap and draw ratio D_R defined as the ratio of die lip gap to film thickness. In a practical process, the drawn film has a free surface, and in addition, large deformation and high strain rate are applied. Therefore, nonlinear

viscoelasticity and processing conditions play an important role on film-casting processability, especially for branched polymers. Recently, many successful simulations using viscoelastic fluid under non-isothermal condition were reported (Seyed and Papanastasiou 1991; Vardarajan and Albert 1993; Rajagopalan 1999; Satoh et al. 2001; Debbaut and Marchal 1995; Smith and Stolle 2003; Shin et al. 2007). The experiment of film casting process for high-pressure process low-density polyethylene (LDPE) and the simulation of the experiment using the Larson model with multiple relaxation times under non-isothermal condition were performed by Satoh et al. (2001). The simulation results showed good correlation with the experimental data. They concluded that high-strain hardening nature of uniaxial elongational viscosity decreased the neck-in of the film. The film-casting experiment using LDPE was carried out to clarify the effect of viscoelastic properties on the neck-in phenomenon (Toft and Rigdahl 2002; Kouda 2008). The obtained results also suggested that the neck-in depended on the ratio of uniaxial elongational viscosity to shear viscosity.

Many researchers have been trying to clarify the mechanism of the neck-in phenomenon. Deformation of a film in air gap was first investigated by Dobroth and Erwin (1986). They derived the model from the experimental data for solidified film. The thickness of the center part decreased in proportion to D_R^{-1} while that of the edge part decreased in proportion to $D_R^{-1/2}$. This result indicated that the film edge was deformed by uniaxial elongation, while the center part was deformed in planar elongation. Kajiwara et al. (2006) suggested relationship between the neck-in and viscoelasticity based on Dobroth and Erwin's model. They investigated the origin of the neck-in phenomenon by using the simulation for various viscoelastic and viscous fluids with various model parameters. The conclusion is that the neck-in is determined by the ratio of uniaxial to planar elongational viscosity rather than the strain hardening nature in uniaxial elongational viscosity.

In this study, the experiment of film casting process for LDPE was performed and the neck-in was measured under wide range of processing conditions for take-up velocity and air gap. Dependence of the neck-in on rheological property was also investigated by using the simulation method. The non-isothermal viscoelastic flow simulation corresponding to the experiment was carried out. The Phan–Thien/Tanner model (PTT model) with multiple relaxation times was used for the simulation. As a result, the simulation results were in good agreement with the experimental data. Based on this simulation method and the theoretical neck-in model, we propose the governing rheological property on the neck-in phenomenon in a film-casting process.

Experiment

Experimental method

The experiment of the film casting process was performed to investigate the effect of processing conditions such as take-up velocity and air gap, and viscoelasticity on neck-in phenomenon. Schematic diagram of the film casting process is shown in Fig. 1. The substrate was supplied between chill and nip roll. The molten polymer was extruded through thin gap of a flat die, and then it was drawn by rotational chill and nip rolls. In this experiment, films with same thickness were produced at various processing conditions. Extrusion rate Q can be described as $Q = W_F H_F V$ at arbitrary take-up velocity. Here, W_F represents the film width, H_F the film thickness, and V the take-up velocity, respectively. Based on the supposition that the edge bead was caused by the neck-in phenomenon (Dobroth and Erwin 1986), we consider that the effect of neck-in on cross section area of a film $W_F H_F$ can be neglected by considering mass conservation condition. According to this assumption, the extrusion rate Q needs to be adjusted to V in order to produce films with same thickness. Consequently, the draw ratio D_R, which is defined as the ratio of thickness of die gap $H_D = 0.8$ mm to film thickness $H_F = 20$ μm, was kept at 40. The processing conditions are summarized in Table 1. Dependence of the neck-in on take-up velocity was measured at the air gap of

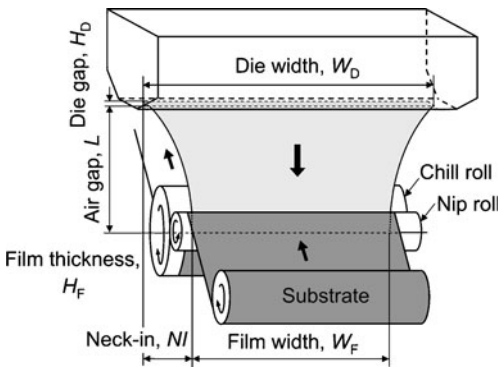

Fig. 1 Schematic diagram of the film casting process. Air gap L was defined as the length between die exit and contact line of a film to chill and nip roll. Neck-in was defined as the length between die width W_D and film width W_F in one side

Table 1 Processing conditions in film casting process

Run number	Temperature (°C)	Die width (mm)	Die gap (mm)	Air gap (mm)	Take-up velocity (m/min)	Flow rate (kg/h)	Draw ratio (–)
1	320	600	0.8	160	80	40	40
2	320	600	0.8	160	120	60	40
3	320	600	0.8	160	190	95	40
4	320	600	0.8	190	120	60	40
5	320	600	0.8	220	120	60	40

160 mm (run number: 1–3). The influence of the air gap on the neck-in was evaluated at the take-up velocity of 120 m/min (run number: 2, 4, and 5).

The neck-in NI was defined as Eq. 1.

$$NI = \frac{1}{2}(W_D - W_F) \tag{1}$$

where W_D represents the die exit width, W_F the final film width, respectively. The neck-in was defined as the difference between the die width and the film width in one side as shown in Fig. 1. In the experiment, the film width at contact line to chill roll was measured by using film products. The air gap L was defined as the length between the die exit and contact line of the film to chill and nip roll.

Materials

Three kinds of conventional LDPE were employed for the film casting experiments. Properties of the LDPE are summarized in Table 2. These LDPE have long chain branch because they were polymerized by a free radical polymerization process under high-pressure condition. Since the PE-A was polymerized by autoclave process, molecular weight distribution M_w/M_n of the PE-A was the widest among these materials, and has more long chain branches than the other LDPEs. On the other hand, as the PE-B and the PE-C were polymerized by tubular process, M_w/M_n of these LDPEs were narrower than that of the PE-A. Strong interaction between polymer chains due to long chain branch and wide M_w/M_n cause the strain hardening phenomenon in elongational flow that plays important role on the neck-in phenomenon.

Simulation

Simulation method

The commercial software POLYFLOW (ANSYS Inc.) based on the finite element method was employed for the simulation corresponding to the experiment of the film casting process. Since aspect ratio of film thickness to width and length can be negligible, about 10^{-4}–10^{-6}, from computational point of view, numerical analysis using three-dimensional model is impracticable. In such a case, the quasi three-dimensional model, so called the film model where physical properties in thickness direction are averaged, was proposed by D'Halewyn et al. (1990). The validity of this model was examined by Satoh et al. (2001). They compared the film thickness distribution in the width direction obtained by the film model simulation with the results of full three-dimensional simulation by Sakaki et al. (1996). As a result, both simulation results were in excellent agreement with each other. Thus, we also employed the film model for the simulation. Most of the references in this study were performed by using the film model.

Material data

The shear viscosity η, the storage modulus G', and the loss modulus G'' were measured by using rotational type rheometer (ARES, TA Instruments) within the range of temperature of 130–190 °C and frequency of 0.1–100 rad/s. The master curve of η, G', and G'' at 130 °C, obtained by the time–temperature superposition rule and empirical rule of Cox and Merz, is shown in Fig. 2. Steady-state η and uniaxial elongational viscosity η_U was measured by using capillary type rheometer (Flowmaster, Malvern Instruments) based on the

Table 2 Properties of the materials for film casting experiment

Materials	*MFR* (g/10 min)	Melt tension (cN)	M_w (kg/mol)	M_w/M_n (–)
PE-A	6.7	2.1	163	9.1
PE-B	4.1	3.3	102	6.6
PE-C	4.3	1.9	85	6.0

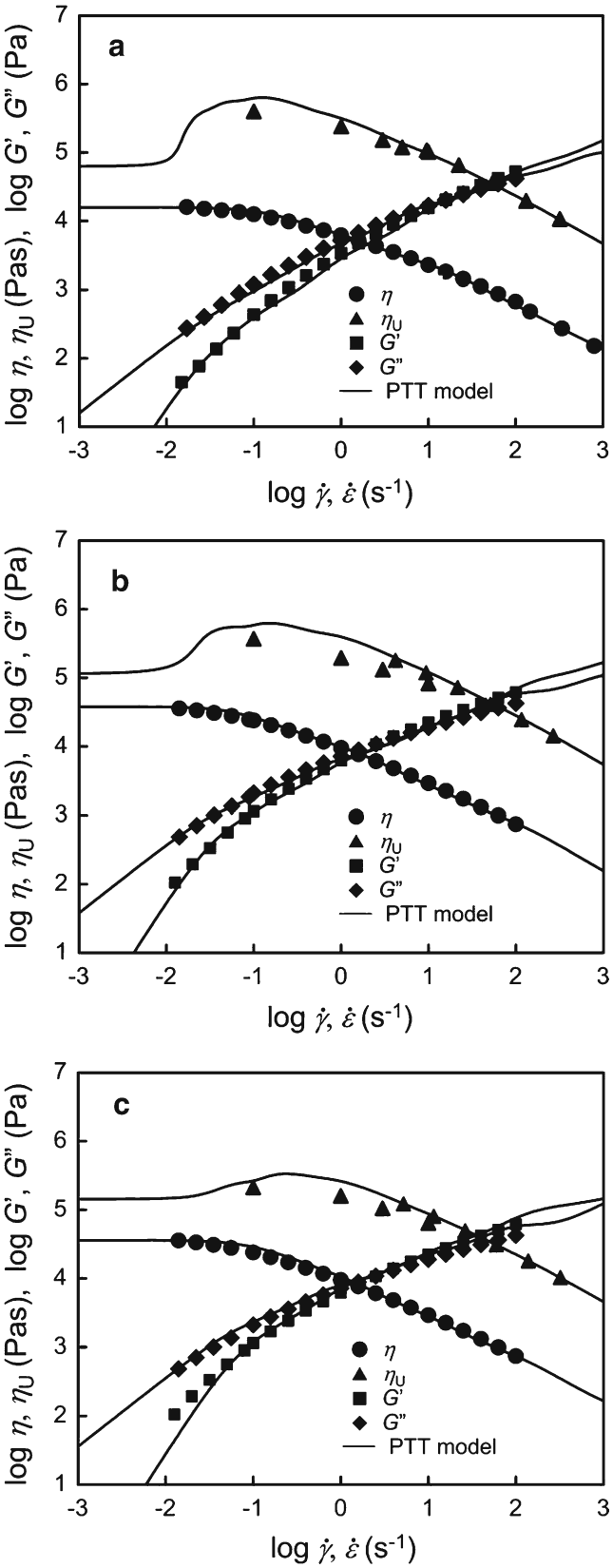

Fig. 2 Viscoelasticities of the materials at 130 °C for **a** PE-A, **b** PE-B, and **c** PE-C. The *symbols* represent experimental data; the *lines* represent prediction of the PTT model

method proposed by Cogswell (1972). The Cogswell method is based on the assumption that the inflow angle, from reservoir to capillary, is constant at any elongational rates. It is considered that the assumption of this method at low elongational rate is not reliable because the inflow angle of LDPE depends on elongational rate due to strain hardening nature. Thus, the Meissner type rheometer (ARES-EVF, TA Instruments) was employed to obtain the data at elongational rate of 6 s^{-1} or less. The maximum value of transient uniaxial elongational viscosity η_U^+ obtained by the Meissner type rheometer was regarded as η_U in the steady state. However, it was not confirmed whether the steady-state value of η_U^+ was obtained successfully or the specimen was broken by necking.

The exponential type of the Phan–Thien/Tanner model (PTT model) was used as a constitutive equation for the simulation. The PTT model was the differential type viscoelastic model derived from the temporary network model. The constitutive equation of the PTT model is shown in Eq. 2.

$$\exp\left[\frac{\kappa\lambda}{\eta}tr\left(\boldsymbol{\tau}\right)\right]\boldsymbol{\tau}+\lambda\left[\left(1-\frac{\xi}{2}\right)\overset{\nabla}{\boldsymbol{\tau}}+\frac{\xi}{2}\overset{\Delta}{\boldsymbol{\tau}}\right]=2\eta D \qquad (2)$$

where η represents the viscosity, $\boldsymbol{\tau}$ the extra stress tensor, $\boldsymbol{D}$ the rate of deformation tensor, λ the relaxation time, κ and ξ the nonlinear parameters, ∇ the upper-convected time derivative, and Δ the lower-convected time derivative, respectively. The parameter κ controls non-linearity in elongational flow. The PTT model can be factorized by considering the temperature dependent law. The viscosity and relaxation time in the PTT model is multiplied by the temperature-dependent law. The Arrhenius law was employed as a temperature dependence of the PTT model.

$$f(T)=\exp\left(\frac{\alpha}{T}-\frac{\alpha}{T_r}\right) \qquad (3)$$

where α represents parameter of temperature dependence, T the material temperature, T_r the reference temperature for which $f(T_r)=1$, respectively. The parameters of the PTT model and the Arrhenius law were obtained by curve fitting of the viscoelasticity within temperature range from 130 to 190 °C. The parameters of the PTT model for the simulation are shown in Table 3. The multiple relaxation times were employed for the simulation to reproduce the measured data over wide range of strain rate. The parameter of α in the Arrhenius law was determined as 6,000. Predictions of the PTT model for the LDPE at 130 °C are shown

Table 3 Parameters of Phan–Thien/Tanner model for the LDPE

Mode	λ	η	κ	ξ
PE-A				
1	35.0	4,000	0.01	0.02
2	15.0	2,600	0.009	0.02
3	5.0	3,200	0.008	0.1
4	1.0	3,800	0.06	0.15
5	0.1	2,000	0.08	0.15
6	0.01	500	0.18	0.25
7	0.001	120	0.3	0.25
PE-B				
1	25.0	20,000	0.03	0.1
2	6.0	8,000	0.02	0.1
3	1.0	7,000	0.04	0.1
4	0.1	1,800	0.07	0.2
5	0.01	800	0.18	0.2
6	0.001	120	0.4	0.2
PE-C				
1	12.0	11,000	0.06	0.1
2	4.0	1,400	0.01	0.1
3	1.0	5,600	0.03	0.1
4	0.1	2,200	0.06	0.2
5	0.01	600	0.15	0.2
6	0.001	150	0.4	0.2

in Fig. 2 with the corresponding experimental data. The constant material properties in molten state of the density ρ of 745 kg/m^3, the specific heat capacity C_p of 3,000 J/(kg·K) and the thermal conductivity k of 0.22 W/(m·K) were imposed into the simulation conditions, respectively.

Results and discussion

Comparison between simulation and experiment

The streamlines of the film obtained by the simulation for the LDPE are shown in Fig. 3. The take-up velocity was 120 mm/min and the air gap was 160 mm. The left side of the figures corresponds to the center of the film, while right side corresponds to the film edge. Since the stream function was indicated at the same intervals, the flow rates between each line are the same. It is understood from the mutually parallel streamlines on the center side that film undergoes planar elongational deformation. On the other hand, the interval of the streamlines in the edge part of the film decreased from die to roll. It is considered that the neck-in phenomenon does not occur at the whole of the film but occurs only at the edge part.

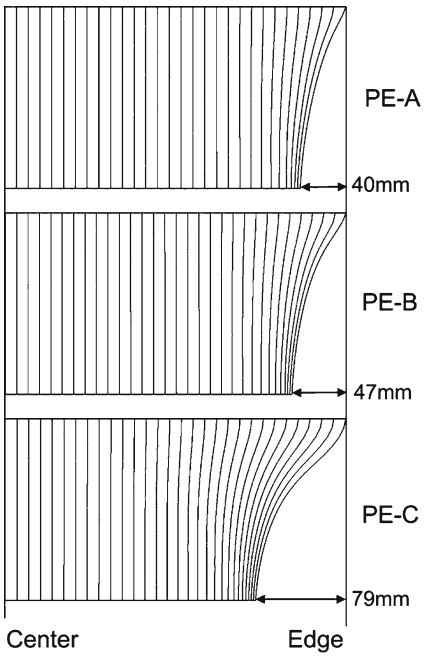

Fig. 3 The streamlines obtained by the simulation for the LDPE at take-up velocity of 120 m/min and air gap of 160 mm

The measured and simulated values of the neck-in are shown in Fig. 4 as a function of take-up velocity at the air gap of 160 mm. The neck-in obtained by the simulation was in good agreement with the corresponding experimental data within the measured range of take-up velocity. The neck-in of all the materials decreased with increasing take-up velocity. The neck-in of the PE-A, which shows the strongest strain hardening of η_U,

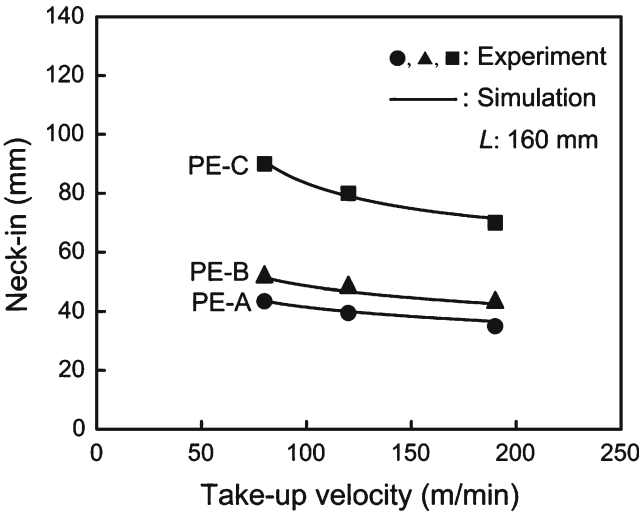

Fig. 4 Relationship between neck-in and take-up velocity for the LDPE at air gap of 160 mm

was the smallest. On the other hand, that of the PE-C, which shows the weakest strain hardening of η_U, was the largest and depended strongly on the take-up velocity. Thus, the strain hardening of η_U depressed the neck-in for the LDPE as well as many studies (Satoh et al. 2001; Debbaut and Marchal 1995; Toft and Rigdahl 2002; Kouda 2008). Since molecular weight of the PE-A is the lowest among the materials, it is considered that molecular weight is not essential factor of the neck-in phenomenon.

Figure 5 shows the variation in the neck-in with various air gaps at the take-up velocity of 120 m/min. The neck-in of each material increased almost linearly with increasing air gap. It is considered that the increase of the air gap gave longer deformation time to the film.

From Figs. 4 and 5, it is confirmed that the simulation could quantitatively reproduce the neck-in phenomenon in the film casting experiment for conventional LDPEs over wide range of processing conditions.

Simulation of the model fluids

The effect of viscoelasticity on the neck-in in film casting process was investigated analytically by using the simulation of the model fluids, based on the idea proposed by Kajiwara et al. (2006). The model fluids which employed the PTT model exhibit specific viscoelasticity due to various combinations of the relaxation times and the nonlinear parameters. Parameters of the PTT model for the model fluids are shown in Table 4. The parameters of the model fluids were chosen to involve weak (model A), medium (model B), and strong (model C) strain-hardening properties. The largest relaxation time λ and nonlinear parameter κ were chosen for the model A, while the smallest λ and κ were chosen for the model C. Parameters for the model B were chosen between the models A and C. The same analysis mesh, boundary conditions, and material properties (ρ, C_p, k) typical of the LDPE were employed for the simulation of the model fluids.

Table 4 Parameters of the model fluids

Mode	λ	η	κ	ξ
Model A				
1	30.0	5,000	0.3	0.01
2	10.0	17,000	0.15	0.01
3	1.0	5,000	0.25	0.02
4	0.1	1,500	0.2	0.02
5	0.01	500	0.2	0.02
6	0.001	100	0.2	0.02
Model B				
1	10.0	12,500	0.3	0.2
2	4.0	8,000	0.05	0.2
3	0.6	4,300	0.07	0.2
4	0.1	2,400	0.07	0.2
5	0.01	800	0.07	0.2
6	0.001	260	0.07	0.2
Model C				
1	7.0	10,000	0.02	0.6
2	3.0	7,000	0.015	0.6
3	0.8	6,400	0.02	0.6
4	0.1	3,000	0.02	0.6
5	0.01	900	0.02	0.6
6	0.001	400	0.02	0.6

Viscoelasticity curves of the model fluids at temperature of 130 °C are shown in Fig. 6. Viscoelasticity curves of the LDPE are also shown for the comparison. The shear viscosity curves of all the model fluids, which exhibited almost same behavior, are close to that of the LDPE B and C. Strain hardening nature of η_U of the model A was the weakest among all the fluids because of the largest non-linear parameter κ. On the other hand, the onset of strain hardening of η_U for the model A was the lowest among the model fluids because of the longest relaxation time λ. Strain hardening of η_U for the model C was the strongest because of the smallest κ, while η_U rose at the highest elongational rate due to the shortest relaxation time. The viscoelasticity of the model B exhibited intermediate behavior between the models A and C. On the other hand, the planar elongational viscosity η_P of all the model fluids exhibited similar behavior with η_U.

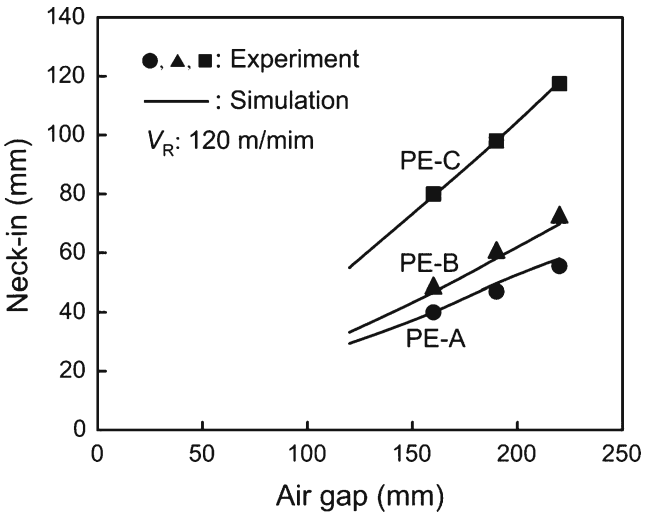

Fig. 5 Relationship between neck-in and air gap for the LDPE at take-up velocity of 120 m/min

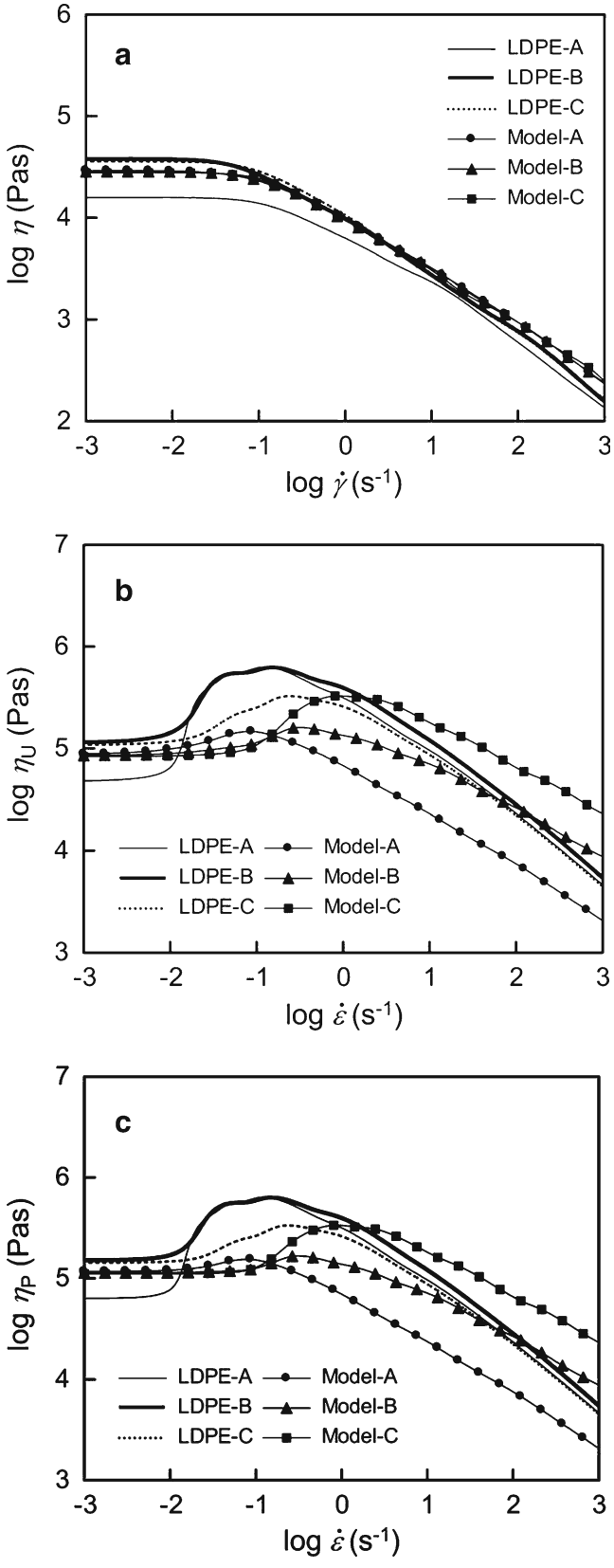

◀ **Fig. 6** Comparison of **a** η, **b** η_U and **c** η_P for the model fluids and the LDPE at 130 °C. The PTT model was employed as the constitutive equation. η of all the model fluids exhibited almost the same behavior. Relaxation times and nonlinear parameters of the model fluids were chosen to involve weak (*Model A*), medium (*Model B*), and strong (*Model C*) elongational thickening properties

In previous papers (Satoh et al. 2001; Debbaut and Marchal 1995; Toft and Rigdahl 2002; Kouda 2008), it was reported that the strain hardening nature of η_U depressed the neck-in. In this study, the neck-in of the LDPE was also depressed by strain hardening of η_U. Here, viscosity ratio η/η_U at the same strain rate was regarded as the reciprocal index of strain hardening of η_U. If the strain hardening nature of η_U is the dominant factor of the neck-in phenomenon, it is expected that the neck-in of all the samples are proportional with viscosity ratio η/η_U. The neck-in data at the take-up velocity of 80, 120, and 190 m/min are shown in Fig. 7 as a function of average viscosity ratio $< \eta/\eta_U >$. Here, predictions of the PTT model were used because quantitative validity of the simulation method in this study was confirmed as discussed above. Since extruded materials undergo a transient process from die exit at $\dot{\varepsilon}$ low to chill roll at high $\dot{\varepsilon}$, the viscosity ratio $< \eta/\eta_U >$ was averaged within the strain rate from 10^{-3} s^{-1} to the maximum rate at each processing conditions. The neck-in of the LDPE increased with increasing $< \eta/\eta_U >$, thus this result agrees well with previous papers (Satoh et al. 2001; Debbaut and Marchal 1995; Toft and Rigdahl 2002; Kouda 2008). In contrast to this result, the neck-in of the model fluids had no relevance to $< \eta/\eta_U >$. The neck-in of the model A, which exhibits the weakest strain hardening nature, was the smallest among the model fluids, while that of the model C, which exhibits the strongest strain hardening nature, was the largest. These results are clearly inconsistent with the results of the LDPE and previous papers. This result suggests that neck-in may correlate with other rheological properties rather than the strain hardening nature of η_U. This will be discussed later by using theoretical model proposed by Shiromoto et al. (2010).

The effect of viscoelasticity on the neck-in phenomenon

Dobroth and Erwin (1986) reported the film deformation type in the sheet extrusion process. It was found from their experiment that the thickness ratio H_F/H_D in the central part was D_R^{-1}, and the ratio on the edge

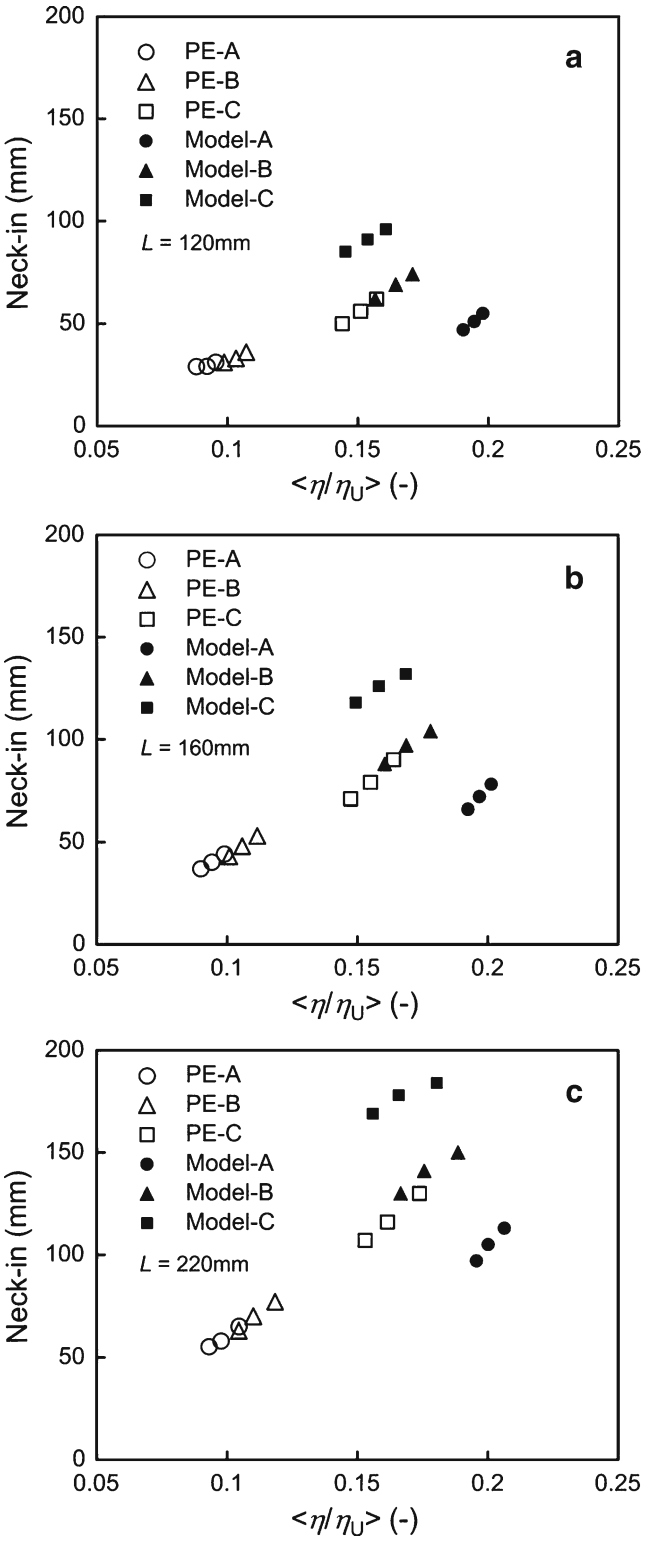

Fig. 7 The neck-in at take-up velocity of 80, 120, and 190 m/min as a function of the viscosity ratio $<\eta/\eta_U>$ at **a** $L = 120$ mm,**b** $L = 160$ mm, and **c** $L = 220$ mm. The $<\eta/\eta_U>$ represents average viscosity ratio within the range from 10^{-3} s^{-1} to the maximum strain rates at each processing conditions

part was $D_R^{-1/2}$. Here, H_F represents the thickness of a film, H_D the gap of a die exit, respectively. This reveals that the central part of a film undergoes planar elongational deformation, while the edge undergoes uniaxial elongational deformation. In addition, there is another interesting paper by Canning and Co (2000). They measured the tension distribution of a film under various D_R. As a result, the film tension in the width direction was almost constant. According to these experimental results, the following mechanism is expected to dominate the neck-in phenomenon. The neck-in is strongly influenced by the balance of the force at planar deformation part and that at uniaxial deformation part in width direction.

Based on the findings shown above, the theoretical model was developed to describe film edge shape as a function of air gap length, that is, neck-in shape (Shiromoto et al. 2010).

$$NI(x) = \left[\int_0^L dx' \int_{x'}^L \frac{\eta_C(x'')\dot{\varepsilon}_C(x'')H_C(x'')}{\eta_E(x'')\dot{\varepsilon}_E(x'')H_E(x'')} dx'' \right]^{1/2} \tag{4}$$

where, x represents axis along take-up direction, subscript of C the center and E the edge of the film, respectively. This equation can be reduced to

$$NI \cong L \left\langle \frac{\eta_C \dot{\varepsilon}_C H_C}{\eta_E \dot{\varepsilon}_E H_E} \right\rangle_L^{1/2} \tag{5}$$

where the operator $\langle\cdot\rangle_L$ represents averaging operation ranging from $x = 0$ to L. This model suggests that the neck-in phenomenon obeys the product of the air gap and the ratio of planar elongational force in the central part to uniaxial elongational force in the edge part. The behavior of above factors in the air gap was investigated from the simulation results to understand the mechanism of the neck-in phenomenon.

The deformation of a film was examined by this simulation method over wide range of D_R. Relationship between H_F/H_D and D_R at the center and the edge is shown in Fig. 8. The thickness ratio of a film at the center H_C/H_D was D_R^{-1}, while that at the edge H_E/H_D was almost $D_R^{-1/2}$ within simulated range of D_R. It was found from Fig. 8 that the thickness ratio H_C/H_E was reduced to constant value $D_R^{-1/2}$ at arbitrary D_R. This result leads us to the conclusion that thickness ratio $\langle H_C/H_E \rangle_L^{1/2}$ slightly affects on the neck-in behavior. Then, elongational rate of the film was examined. Distribution of elongational rate along the center $\dot{\varepsilon}_C$ and the edge $\dot{\varepsilon}_E$ are shown in Fig. 9. These strain rates increased steeply near chill roll. Since both behaviors

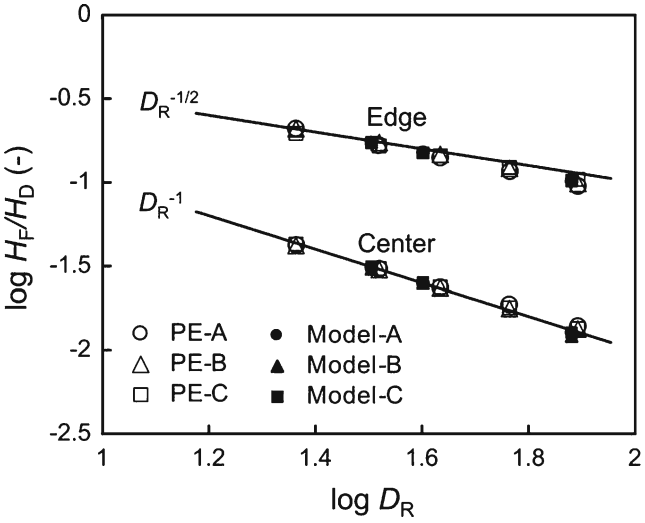

Fig. 8 The thickness ratio of the film H_F to the die gap H_D as a function of draw ratio D_R. The *line* of D_R^{-1} represents the thickness ratio in planar elongational deformation, and the *line* of $D_R^{-1/2}$ represents the thickness ratio in uniaxial elongational deformation, respectively

were similar to each other, the ratio $\langle \dot{\varepsilon}_C/\dot{\varepsilon}_E \rangle_L^{1/2}$ can be approximated to unity. Therefore, it seems reasonable to consider that the effect of H and $\dot{\varepsilon}$ on the neck-in could be negligible. The remaining factors in the neck-in model, Eq. 5, are L and the viscosity ratio η_C/η_E.

From rheological point of view, it is considered that the neck-in phenomenon originates from η_P/η_U because the η_P is expected to play an important role on the planar film deformation at the central part, while η_U may affect on the uniaxial elongational deformation at the film edge. Relationship between the neck-in and the averaged viscosity ratio $< \eta_P/\eta_U >$ at various take-up velocities and air gaps obtained from the simulation is shown in Fig. 10. The η_P/η_U was averaged in the range from 10^{-3} s^{-1} to the maximum strain rate at each processing conditions to include the transient deformation history from die exit to chill roll. Not only neck-in of the LDPE but also that of the model fluids were in good agreement with the average viscosity ratio $< \eta_P/\eta_U >$. This relationship has a dependence on the air gap L as expected from Eq. 5.

The neck-in model (Eq. 5) could be reduced to Eq. 6 by eliminating the effect of thickness and strain rate on the neck-in.

$$NI \cong L \left\langle \frac{\eta_P}{\eta_U} \right\rangle_L^{1/2} \tag{6}$$

Equation 7 is obtained by dividing Eq. 6 by L.

$$NI^* = \frac{NI}{L} \cong \left\langle \frac{\eta_P}{\eta_U} \right\rangle_L^{1/2} \tag{7}$$

The neck-in NI^*, normalized by the air gap L, depends only on the ratio of planar elongational viscosity to uniaxial elongational viscosity. Here, let us consider the

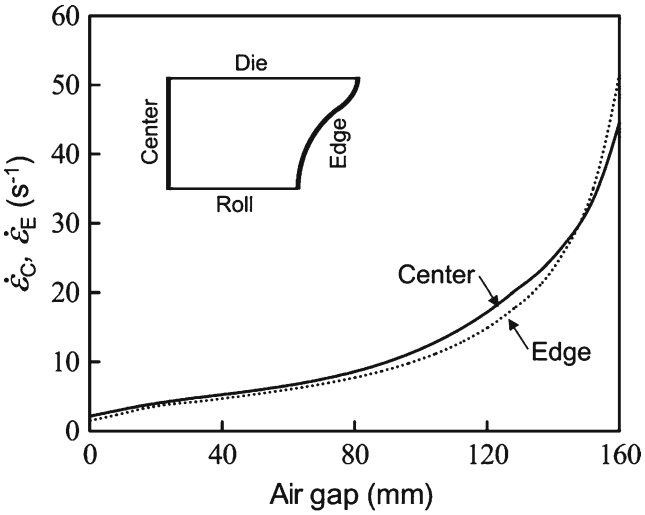

Fig. 9 Elongational rate in air gap form die to chill roll. The *solid line* represents elongational rate along the center of the film, and the *dotted line* represents that along the edge

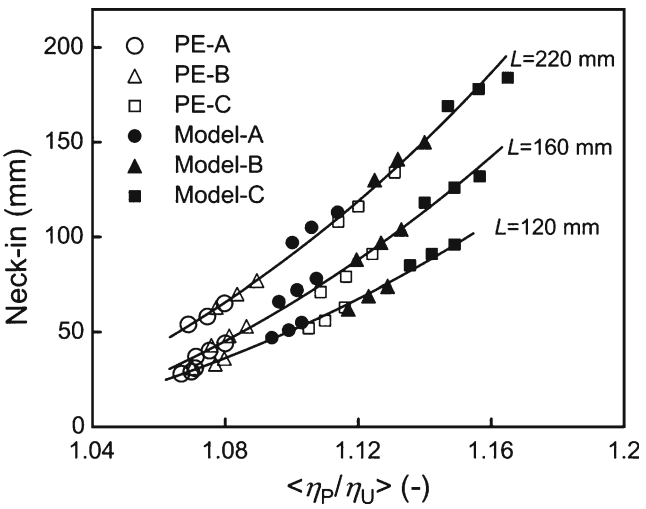

Fig. 10 Relationship between neck-in and the viscosity ratio $< \eta_P/\eta_U >$ obtained by the simulation for various processing conditions. The $< \eta_P/\eta_U >$ represents average viscosity ratio within the range from 10^{-3} s^{-1} to the maximum strain rates at each processing conditions

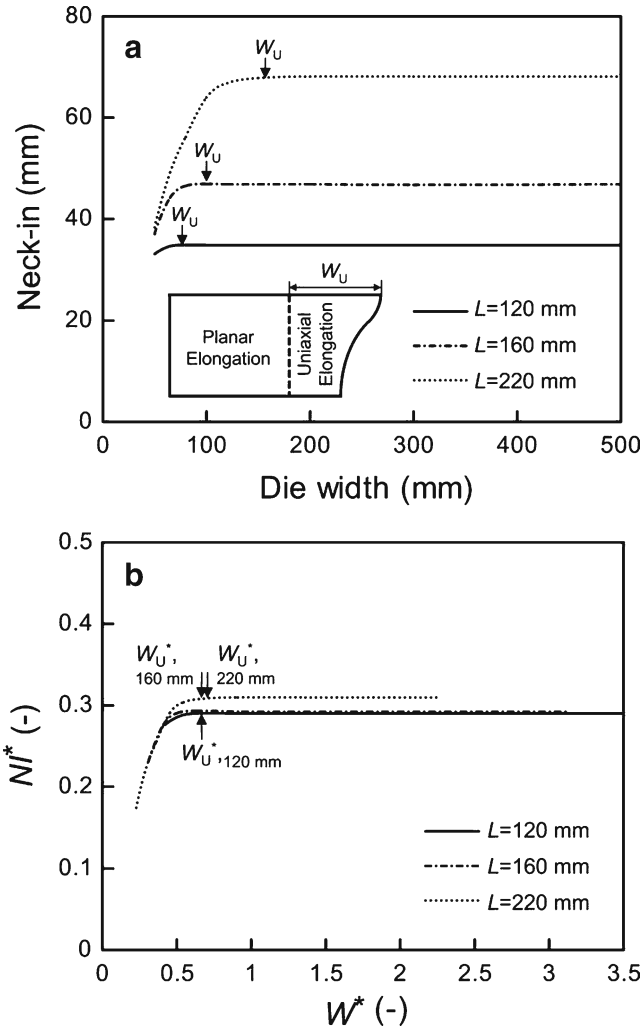

Fig. 11 **a** Relationship between neck-in and die width, **b** Normalized neck-in as a function of normalized die width. Reference length is air gap

effect of the air gap on the neck-in. The neck-in NI of the PE-B at various air gaps is shown in Fig. 11a as a function of die width W. The die width has no influence on the neck-in except for the short die width region. The width of uniaxial elongational deformation part W_U is defined as the difference between die width and planar elongational deformation part width as shown in Fig. 11a. Actually, the border of planar and uniaxial elongational deformation part is determined as the position that thickness is more than 105% of planar deformation part. The W_U increased linearly with increasing air gap as well as the neck-in as shown in Fig. 5. The neck-in showed no dependence on the die width when the die width was longer than W_U. It is considered that the neck-in phenomenon occurs only in the uniaxial elongational deformation part; therefore, the planar deformation part plays no role on the neck-in phenomenon.

The variation of the neck-in NI^* with the die width W^* normalized by the air gap is shown in Fig. 11b. The NI^* shows no dependence on not only die width but also air gap. This can be understood from Fig. 5 that neck-in depends almost linearly on air gap. The W_U^* at various air gap also has no dependence on die width by the normalization by the air gap. It is expected from results shown above that film edge shape at various air gaps are analogous relationship. However, the decrease in the strain rate due to the increase in the air gap caused a small increase in the neck-in. It is, therefore, considered that above relation is applicable within the limited range of air gap. Thus, the dependence of the neck-in on film geometry such as die width and air gap could be eliminated by the normalization of the air gap.

Let us return to the discussion about Eq. 7 again. The NI^* is shown in Fig. 12 as a function of average viscosity ratio $< \eta_P/\eta_U >$. The master curve, therefore, was obtained from the relationship between the neck-in normalized by the air gap and the viscosity ratio η_P/η_U. The model fluids for which the neck-in showed no dependence on $< \eta/\eta_U >$ was on the same master curve as well as LDPE. Thus, the neck-in normalized by the air gap, for industrial LDPE and the model fluids, were in quantitative agreement with $< \eta_P/\eta_U >$ under wide range of processing conditions such as air gap and

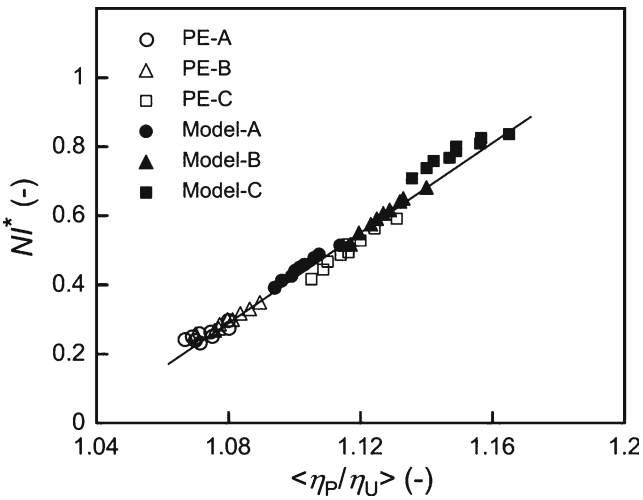

Fig. 12 Relationship between neck-in normalized by air gap and the viscosity ratio $< \eta_P/\eta_U >$ obtained by the simulation under various materials and processing conditions

take-up velocity. Moreover, this result proves clearly that the neck-in model expressed in Eq. 5 describes the neck-in phenomenon properly. It is confirmed that the neck-in is controlled by the viscoelasticity, i.e., the ratio of planar elongational viscosity to uniaxial elongational viscosity. It is expected that further research on planar elongational viscosity would evidence our model about the effect of viscoelasticity on the neck-in phenomenon.

Conclusion

In this study, the experiment and the non-isothermal viscoelastic flow simulation of the film casting process were performed. It was confirmed that simulation results were in good quantitative agreement with the experimental data for various industrial LDPE over wide range of processing conditions. The effects of viscoelasticity on the neck-in were investigated by using simulation results of the LDPE and the model fluids exhibiting specific viscoelasticity. As a result, it was found that the strain hardening nature of uniaxial elongational viscosity was not only dominant factor of the neck-in phenomenon. The neck-in phenomenon was examined by using the theoretical model based on the force balance and deformation type of a film. As a result, the following findings were obtained that the neck-in was determined by the product of the air gap and the force balance between the central and the edge part of a film. The central part undergoes planar elongational deformation, while the edge part undergoes uniaxial elongational deformation. These results led us to the conclusion that neck-in was proportional to the viscosity ratio η_P/η_U and the air gap. In addition, the neck-in normalized by the air gap exhibited constant value because the neck-in correlated linearly with air gap. The master curve, therefore, was obtained from the relationship between the neck-in normalized by the air gap and the viscosity ratio η_P/η_U at wide range of processing conditions of various samples.

References

Barq P, Haudin JM, Agassant JF (1992) Isothermal and anisothermal models for cast film extrusion. Int Polym Process 12:334–344

Canning K, Co A (2000) Edge effects in film casting of molten polymers. J Plast Film Sheeting 16:188–203

Cogswell FN (1972) Measuring the extensional rheology of polymer melts. Trans Soc Rheol 16:383–403

Debbaut B, Marchal JM (1995) Viscoelastic effects in film casting. Z Angew Math Phys 46:679–698

D'Halewyn S, Agassant JF, Demay Y (1990) Numerical simulation of the cast film process. Polym Eng Sci 30:335–340

Dobroth T, Erwin L (1986) Causes of edge beads in cast films. Polym Eng Sci 26:462–467

Ito H, Doi M, Isaki T, Takeo M (2003) A model of neck-in phenomenon in film casting process. Nihon Reoroji Gakkaishi 31:157–163

Kajiwara T, Yamamura M, Asahina T (2006) A model of neck-in phenomenon in film casting process. Nihon Reoroji Gakkaishi 34:97–103

Kouda S (2008) Prediction of processability at extrusion coating for low-density polyethylene. Polym Eng Sci 49:1094–1102

Rajagopalan D (1999) Impact of viscoelasticity on gage variation in film casting. J Rheol 43:73–83

Sakaki K, Katsumoto R, Kajiwara T, Funatsu K (1996) Three-dimensional flow simulation of a film-casting process. Polym Eng Sci 36:1821–1831

Satoh N, Tomiyama H, Kajiwara T (2001) Viscoelastic simulation of film casting process for a polymer melt. Polym Eng Sci 41:1564–1579

Seyed MA, Papanastasiou TC (1991) Film casting of viscoelastic liquid. Polym Eng Sci 31:67–75

Shin DM, Lee JS, Kim JM, Jung HW, Hyun JC (2007) Transient and steady-state solutions of 2D viscoelastic nonisothermal simulation model of film casting process via finite element method. J Rheol 51:393–407

Shiromoto S, Masutani Y, Tsutsubuchi M, Togawa Y, Kajiwara T (2010) A neck-in model in extrusion lamination process. Polym Eng Sci 50:22–31

Smith S, Stolle D (2003) Numerical simulation of film casting using an updated Lagrangian finite element algorithm. Polym Eng Sci 43:1105–1122

Sollogoub C, Demay Y, Agassant JF (2003) Cast film problem: a non isothermal investigation. Int Polym Process 18:80–86

Toft N, Rigdahl M (2002) Extrusion coating with metallocene-catalysed polyethlenes. Int Polym Process 17:244–253

Vardarajan RI, Albert C (1993) Film casting of a modified Giesekus fluid: a steady-state analysis. J Non-Newton Fluid Mech 48:1–20